Journal of *Marine Science and Engineering*

MDPI

Article

Design and Theoretical Analysis of a MAC Protocol for the Korean Tsunami and Earthquake Monitoring System

Sung Hyun Park and Taeho Im *

Department of Information and Communication Engineering, Hoseo University, Asan 42409, Republic of Korea; shpark@hoseo.edu

* Correspondence: taehoim@hoseo.edu

Abstract

Tsunamis and submarine earthquakes pose severe risks to coastal regions, demanding rapid and reliable monitoring systems. While the Deep-ocean Assessment and Reporting of Tsunamis (DART) system has been globally deployed, its dependence on pressure sensors and one-to-one communication limits its applicability to the Korean East Sea. This paper introduces the Korean Tsunami and Earthquake Monitoring System, which integrates seafloor seismometers and proposes a dedicated Medium Access Control (MAC) protocol optimized for multi-node underwater acoustic communication. The study performs a comprehensive analytical derivation of closed-form expressions for channel utilization and energy consumption under diverse node configurations and acoustic conditions. The analytical results confirm that the proposed MAC protocol maintains stable performance, supports multi-node operation, and enables long-term monitoring within the limited energy budget of underwater devices. The derived results also provide practical design implications for underwater network planning, including guidelines on node placement, frame duration, and control packet timing for efficient data delivery. Although empirical validation remains as future work, the findings establish theoretical benchmarks and engineering insights for the design of next-generation underwater monitoring systems tailored to Korean coastal environments.

Keywords: battery life analysis; earthquake monitoring system; MAC protocol; tsunami early warning; tsunami monitoring system; underwater acoustic networks

1. Introduction

Tsunamis are among the most devastating natural disasters faced by humankind. The 2004 Indian Ocean tsunami and the 2011 Great East Japan tsunami are representative examples, both of which resulted in catastrophic losses. These two events are among the most destructive in history, yet tsunamis of varying scales continue to occur worldwide [1]. Although various causes such as submarine volcanic eruptions and submarine landslides may trigger tsunamis, undersea earthquakes account for approximately 80% of tsunami occurrences [2]. Consequently, while the development of tsunami early warning systems is critical, the monitoring and prediction of submarine earthquakes are equally important for enhancing tsunami forecasting capabilities.

In addition to deep-ocean pressure sensors, several complementary sensing technologies have been investigated for tsunami-related ocean monitoring. Among them, high-frequency surface wave radars (HFSWRs) deployed along coastlines can observe large-scale variations in sea surface conditions by analyzing Bragg line characteristics in

Check for updates

Academic Editor: Gianluca Quarta

Received: 24 November 2025
Revised: 16 December 2025
Accepted: 17 December 2025
Published: 22 December 2025

Copyright: © 2025 by the authors. Licensee MDPI, Basel, Switzerland. This article is an open access article distributed under the terms and conditions of the Creative Commons Attribution (CC BY) license.

range–Doppler maps. Owing to surface wave propagation, such radar systems are capable of monitoring ocean areas extending over several hundred kilometers from the coast, and thus may contribute to the early detection of abnormal sea states associated with tsunami events [3–5]. Nevertheless, HFSWRs primarily provide indirect surface observations and cannot replace direct deep-ocean measurements for tsunami confirmation. Recent studies on high-resolution HFSWRs have shown that, due to their improved range–Doppler resolution, Bragg lines can be detected at greater distances compared to conventional HFSWR systems, which represents a key advantage in wide-area ocean monitoring.

The Deep-ocean Assessment and Reporting of Tsunamis (DART) system, originally developed by the National Oceanic and Atmospheric Administration (NOAA), has become the most widely adopted tsunami early warning system worldwide. As illustrated in Figure 1, the DART system consists of a buoy and a tsunameter [6], which employs underwater acoustic wireless communication between them. It has evolved through four generations: the initial versions were primarily deployed in the Pacific Ocean, including Alaska and Hawaii, with the primary objective of detecting tsunamis at long distances and issuing early warnings. With the introduction of DART II, the system was extended to mid-range coastal regions such as the Indian Ocean and South America, thereby serving as a critical component of the international tsunami warning infrastructure. DART stations are strategically located along the "Ring of Fire," where earthquakes occur most frequently [7].

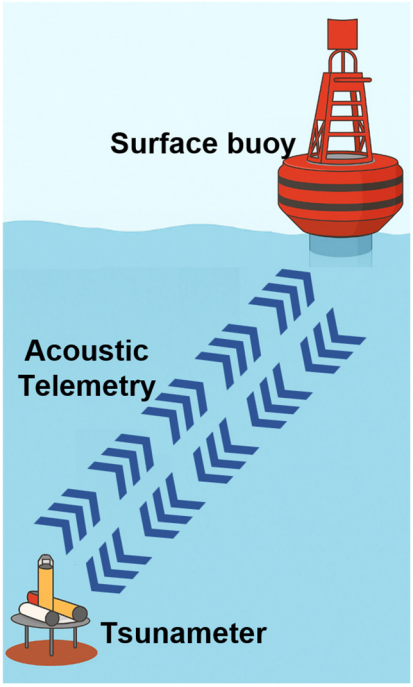


Figure 1. The DART II system consists of a surface buoy and a bottom pressure recorder (tsunameter), connected through acoustic wireless communication and relaying data via satellite to a tsunami warning center [6].

However, no DART stations are deployed in the seas surrounding the Korean Peninsula [7]. This absence is primarily due to the relatively low frequency and smaller magnitude of tsunamis in Korea compared with countries located along the Ring of Fire. In South Korea, only three tsunami events have been recorded—occurring in 1983, 1993, and 2024—since systematic observations began. Among them, one fatality occurred in 1983, caused by an earthquake in the Sea of Japan [8]. Although the impact of tsunamis in Korea has been relatively minor compared with that in Ring of Fire countries, the region

remains within the potential tsunami-affected zone. More critically, both the frequency and magnitude of earthquakes occurring in the East Sea have shown an increasing trend [9].

Accordingly, the Korean government has deployed 137 seismic observation stations nationwide, including three dedicated tsunami observation stations [10]. All of these stations rely on cable-based (wired) communication. As a result, due to the physical distance limitations of wired connections, the stations are installed exclusively along the coasts of the mainland and islands. The disadvantages of cable-based deployment extend beyond distance limitations to include high installation costs (e.g., cable burial) and substantial maintenance requirements. These limitations highlight the necessity of establishing a new, wireless-based observation and warning infrastructure.

To address these limitations, the Korea Institute of Geoscience and Mineral Resources (KIGAM) [11] has initiated a national project to develop and deploy an indigenous tsunami early warning system in Korean waters. The project is entitled "Real-Time Monitoring Technology for Submarine Disasters" [12]. In this paper, we propose a higher layer protocol tailored to the requirements of this new project and analyze its performance in comparison with the existing DART system. Similarly to DART, the system is designed to operate through an acoustic wireless network while simultaneously serving as an integrated seismic and tsunami observation platform. This study focuses exclusively on contrasting the proposed system with the well-established DART system as a baseline, in order to demonstrate its applicability to the Korean East Sea. The contributions of this paper are threefold:

- System proposal: This study proposes the Korean Tsunami and Earthquake Monitoring System (KTEMS), a buoy-centered 1:3 acoustic wireless communication system designed to establish a national-scale tsunami and earthquake monitoring infrastructure optimized for the Korean East Sea.
- Protocol design: A dedicated Medium Access Control (MAC) protocol is proposed to enable efficient and reliable communication among multiple underwater nodes, overcoming the one-to-one communication limitation of the DART system.
- Theoretical evaluation: The proposed MAC protocol is analytically evaluated with respect to channel utilization and energy consumption. These results establish theoretical benchmarks for long-term deployment and provide a foundation for future sea trial validation.

The remainder of this paper is organized as follows. Section 2 provides the necessary information on the DART system. Section 3 defines the system requirements, and Section 4 presents the system design. Section 5 analyzes the predicted theoretical performance of the proposed system. Finally, Section 6 concludes the paper.

2. DART System Overview

The DART system has evolved through four generations [13]. The first generation was designed for long-range communication, primarily targeting early warnings for distances greater than 1000 km [14]. Beginning with the second generation, the system was extended to cover mid-range distances of less than 1000 km [14], thereby enabling both mid- and long-range coverage. The third generation introduced a simplified version with easier installation, while the fourth generation incorporated comprehensive upgrades in algorithms, functionality, hardware, modems, and batteries.

As shown in Figure 1, the DART system employs a one-to-one communication scheme in which a single buoy is wirelessly connected to a single tsunameter. The tsunameter, as illustrated in Figure 2, consists of a pressure sensor, modem, battery, and onboard computer [15]. It is anchored flat on the seafloor, and the embedded pressure sensor measures the water pressure, i.e., the weight of the overlying water column. The measured signal is output from the pressure sensor as a square wave, which is then counted by a

frequency counter. The counter samples the data once every 15 s [15–18] and transfers the values to the onboard computer, where an algorithm converts the measurements into sea-level height and stores the results. In the DART system, this sampling interval reflects a design trade-off between temporal resolution, signal stability, data volume, and power consumption for long-term deep-ocean monitoring, and is not a parameter defined in this study.

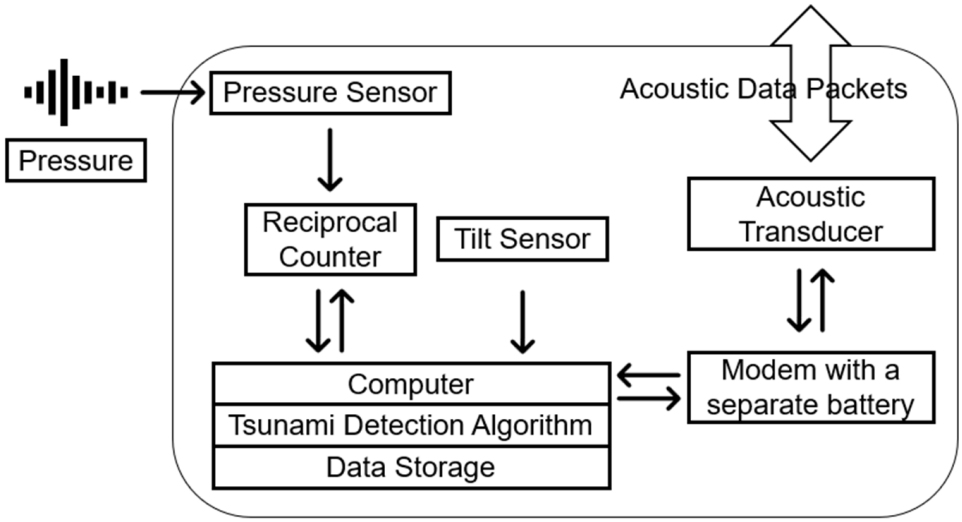


Figure 2. Block diagram of the tsunameter illustrating its main components, including pressure sensor, tilt sensor, onboard computer, modem, acoustic transducer, and batteries [15].

The recorded pressure measurements are converted into equivalent sea-level height, also referred to as water-column height information, by assuming a constant linear relationship between pressure and water height (1 psi = 670 mm of water) [15]. For the purposes of tsunami detection, the errors introduced by neglecting variations in water density and gravitational acceleration are not significant, since the analysis relies on relatively small pressure changes associated with tsunami waves rather than absolute water depth.

The onboard computer transmits the stored information to the buoy via wireless communication. Because the buoy and tsunameter operate in a one-to-one communication scheme, higher layer multifunction protocols are not required. Instead, the system utilizes the XMODEM protocol to transmit data at predetermined intervals.

3. System Requirements

The project initiated by KIGAM is divided into four research units. KIGAM defines the project scope and oversees project management. The other three groups are responsible for different technical domains: one develops underwater seismometers capable of measuring earthquakes; another addresses the physical layer and communication aspects. The last group—corresponding to the focus of this paper—handles higher layer protocol design. Section 3 reviews the requirements of each group and discusses their impact on the proposed protocol design.

3.1. Project Requirements (1:3 Communication)

The NOAA tsunami early warning system, as illustrated in Figure 3, requires not only the information transmitted from the DART system but also data collected from a variety of other sensors [15]. NOAA operates 1142 buoys [7], including DART stations as well as other environmental monitoring stations deployed across the oceans and along coastlines, some of which are cable-connected coastal observatories. The primary motivation for collecting such extensive environmental data is to reduce the probability of false tsunami warnings.

False alarms not only degrade system credibility but also impose significant economic and physical risks during evacuations. For example, a false tsunami warning issued in Hawaii in 1986 caused the dismissal of all state employees and triggered massive traffic congestion, leaving cars gridlocked in evacuation zones. The State of Hawaii estimated that this false alarm cost approximately 41 million USD [19].

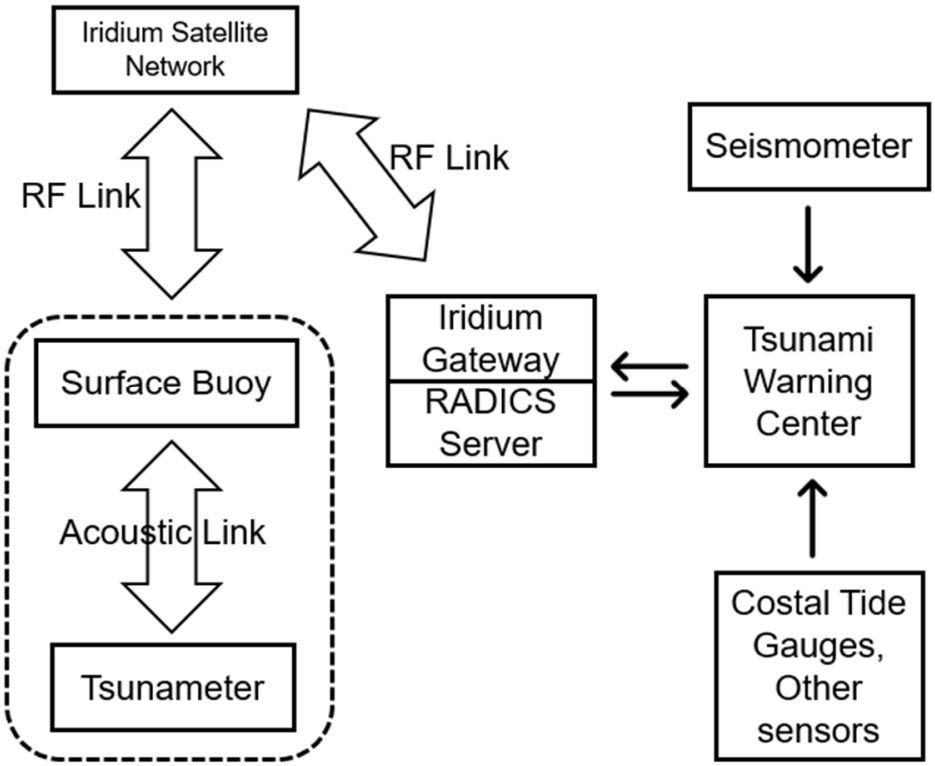


Figure 3. System configuration of the NOAA tsunami early warning system, integrating data from DART systems and other sensors for centralized processing at the Tsunami Warning Center [15].

However, the sea area surrounding the Korean Peninsula is relatively limited, making a DART-style deployment of widely separated, independent environmental observation stations inefficient. Therefore, KIGAM proposes KTEMS supporting a 1:3 acoustic wireless communication scheme, in which a single buoy communicates with three nodes. Among these, one node is a seismometer, while the remaining two nodes are environmental sensors. This feature represents the key distinction between the DART system and KTEMS, and constitutes the central focus of this paper. The use of multiple nodes necessitates the development of a protocol design more advanced than XMODEM.

As shown in Figure 1, the DART system employs a one-to-one communication scheme in which a single buoy is wirelessly connected to a single tsunameter. The rationale for defining DART as a 1:1 communication system is to ensure robust data transmission [20]. Due to considerations such as energy consumption, system complexity, and maintenance, NOAA does not employ one-to-multiple DART configurations for operational deployment, restricting them to research purposes only. In KTEMS, however, a one-to-three communication scheme is adopted, enabling a single buoy to manage multiple seafloor nodes within its coverage area. To guarantee timely and reliable data transmission under this configuration, the buoy is equipped with two independent receivers, each operating at a different frequency.

The DART system is designed as a medium- to long-range early warning system, and its objective is to ensure that an alert reaches the data center within three minutes of tsunami detection [21]. In contrast, KTEMS targets a relatively smaller body of water;

therefore, the first alert must reach the data center within several tens of seconds, as the exact timing requirement is currently under determination by KIGAM. The details of this requirement are closely related to the type of data generated by the seismometer, which will be further explained in the following sections.

3.2. Seismometer Requirements

In the DART system, tsunami early warning relies on a seafloor tsunameter equipped with a pressure sensor. The sensor measures the weight of the overlying water column and converts it into the corresponding water column height. This data is then wirelessly transmitted to the surface buoy and relayed to the onshore data center. Because tsunami waves travel more slowly than seismic waves, they arrive at the tsunameter later; however, the exact time gap varies with the instrument's location. For example, during the Ms 7.6 earthquake in the Gulf of Alaska on 6 March 1988, the tsunami waves were recorded approximately one hour after the seismic waves [14].

In contrast, KTEMS replaces the pressure-based tsunameter of the DART system with a seismometer to achieve faster alerts. Because KTEMS targets short-range early warnings, it requires significantly lower latency. Seismometers can detect seismic waves that arrive much earlier than tsunami waves; therefore, they are particularly suitable for rapid tsunami detection. Accordingly, KTEMS installs seismometers on the seafloor to minimize alert latency and enable prompt responses.

Unlike DART, which transmits only water-column height information, KTEMS seismometers record three-axis (x, y, and z) ground motion across a wide frequency band [22]. They capture various phenomena ranging from tides and earthquake-induced motion to ambient biological and anthropogenic noise [23]. The seismometer response is represented by one real and several complex components, numerically expressed as a combination of multiple real values [24]. Consequently, each seismometer generates substantially larger data volumes than the DART tsunameter. For this project, the raw data generated by the seismometer can reach up to 4096 bits per second, resulting in a packet size of approximately 5000 bits when redundant bits are included. Accordingly, this large data volume imposes critical constraints on both physical-layer design and protocol development.

3.3. Physical Layer Requirements

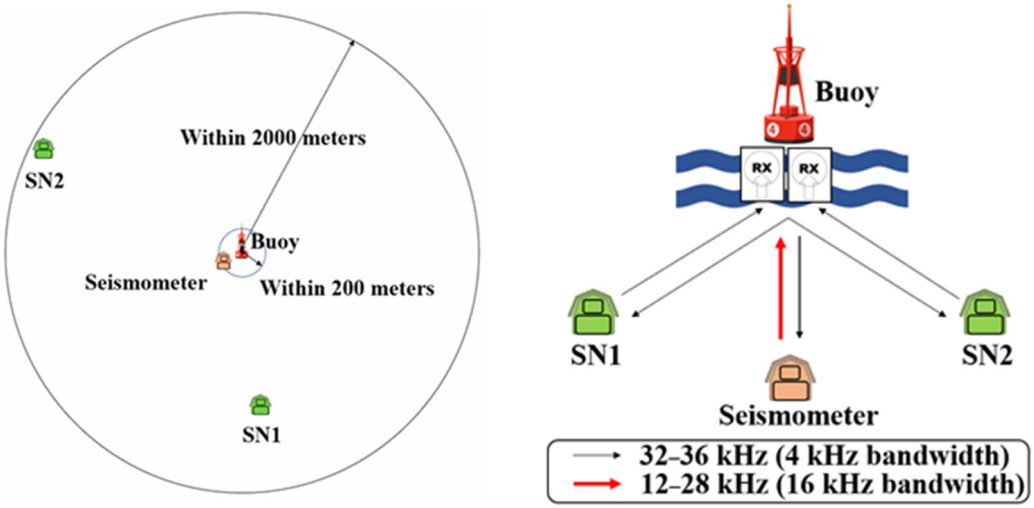
Underwater acoustic wireless communication is fundamentally limited by distance-dependent bandwidth, which reduces the achievable channel capacity. This characteristic imposes a critical constraint on the design of underwater communication ranges.

In this project, the deployment geometry, including the buoy-to-node distances, was specified in advance by the Korea Institute of Geoscience and Mineral Resources (KIGAM) based on the bathymetric characteristics of the Korean East Sea and the spatial distribution of historically observed submarine earthquakes. Accordingly, the communication system was designed to satisfy these predetermined distance requirements rather than being optimized to maximize transmission range.

To satisfy the 5000 bps data rate requirement specified in Section 3.2, the research group responsible for the physical layer and underwater communication conducted extensive sea experiments [25–30]. The experimental results indicate that the channel carrying seismometer data must utilize a 16 kHz bandwidth in the 12–28 kHz frequency range, with a maximum buoy-to-node transmission distance of 200 m to ensure stable communication. This distance should therefore be interpreted as a deployment-driven design constraint rather than a fundamental communication limit. Communication at greater distances is not excluded in principle but is outside the scope of the targeted system configuration considered in this study. In contrast, environmental data are assumed to have relatively

smaller volume requirements, and thus can be transmitted over a 4 kHz bandwidth in the 32–36 kHz frequency range, allowing buoy-to-node communication distances of up to 2000 m.

Sensor Node 1 (SN1) indicates the node located closer to the buoy, whereas Sensor Node 2 (SN2) is positioned farther away. As shown in Figure 4a, each node communicates with the buoy in a single-hop configuration. Considering that the DART system operates in the 15–18 kHz frequency band [14], it is evident that KTEMS exploits a comparatively wider bandwidth to accommodate large-volume data transmission. As illustrated in Figure 4b, two separate receiver configurations necessitate the use of two independent receivers in KTEMS to ensure robust delivery of high-volume data.



(**a**) (**b**)

Figure 4. KTEMS physical layer requirements: (**a**) Deployment range of the buoy, seismometer, and sensor nodes (SN1 within 200 m and SN2 within 2000 m from the buoy); (**b**) Frequency allocation for underwater communications: seismometer data transmitted in the 12–28 kHz band (16 kHz bandwidth) and environmental data transmitted in the 32–36 kHz band (4 kHz bandwidth).

To ensure reliable transmission, network-wide time synchronization and initialization must be performed in advance. In the proposed system, all underwater nodes, including the seismometer, SN1, and SN2, are fixed and bottom-mounted, and their deployment locations are predetermined. Prior to deployment, time synchronization is performed onshore using wired connections and GPS-based references as part of the installation procedure, allowing all nodes to start operation with a common initial time reference. During data transmission, slot-level time alignment among the buoy, seismometer, SN1, and SN2 is assumed for MAC operation. To assist in maintaining this alignment after deployment, the buoy periodically transmits control packets at the beginning of each frame, which provide a timing reference for the underwater nodes and help compensate for gradual clock drift. Furthermore, it is assumed that the buoy and all nodes share the same positional information.

4. KTEMS Protocol Design

The requirements presented in Section 3 have an impact on the protocol design of KTEMS. For example, one critical requirement is that the communication distance from the seismometer to the buoy (max 200 m) differs by more than an order of magnitude compared with that from the environmental sensors to the buoy (max 2000 m). When nodes with significantly different communication ranges coexist within the same underwater network, the inherently slow propagation delay of acoustic signals must be carefully addressed at the protocol layer to ensure efficient channel utilization. Based on these requirements,

Section 4 presents the detailed design of KTEMS. To translate the physical-layer constraints identified in Section 3 into MAC-level timing rules, we first establish a simplified signal and channel model.

4.1. Signal Channel Model

This subsection presents a simplified signal and channel model for the underwater acoustic network considered in this study. The objective of this model is not to optimize physical-layer signal processing, but to identify the dominant physical constraints that directly affect MAC-level timing design and performance analysis.

A key distinguishing characteristic of underwater acoustic communication is the low propagation speed of sound in water. Unlike terrestrial radio systems, where propagation delay is typically negligible, acoustic signals propagate at approximately $c \approx 1500\ m/s$, resulting in substantial and distance-dependent propagation delays. The one-way propagation delay between a transmitter and receiver separated by distance d is therefore expressed as

$$\text{Propagation delay} = d/c. \tag{1}$$

As a consequence, even moderate communication distances introduce significant delays, leading to long round-trip times. This property makes instantaneous collision detection impractical and fundamentally limits the applicability of contention-based MAC protocols that rely on carrier sensing or rapid feedback.

In a multi-node underwater acoustic network, these effects are further amplified when multiple sensor nodes communicate with a common buoy from different distances. Packets transmitted at different times may arrive at the receiver simultaneously due to unequal propagation delays, causing collisions that depend not only on transmission timing but also on node geometry. This distance-dependent arrival uncertainty significantly increases the complexity of MAC design.

Moreover, the combination of long propagation delays and limited available bandwidth results in high retransmission overhead, as acknowledgment signals also suffer from long delays. Frequent retransmissions therefore incur substantial energy consumption, which is particularly critical for battery-powered underwater nodes intended for long-term autonomous operation.

These characteristics imply that MAC protocols designed for terrestrial wireless networks cannot be directly applied to underwater acoustic environments. Instead, the MAC protocol must explicitly account for propagation-delay differences among nodes to ensure non-overlapping packet arrivals at the buoy. Consequently, the MAC design problem is transformed into a delay-constrained scheduling problem rather than a conventional random-access problem.

Based on these signal and channel characteristics, this study adopts a packet-level abstraction for MAC analysis. Detailed physical-layer processes, such as modulation, coding, and channel estimation, are not explicitly modeled. Instead, the channel model is used to justify MAC-level assumptions related to long propagation delay, distance-dependent arrival timing, and the necessity of scheduled transmissions.

Accordingly, the core challenge addressed in this study lies not in physical-layer signal processing, but in coordinating transmission timing among multiple nodes under severe and distance-dependent propagation delays. Based on these channel characteristics, the MAC design problem reduces to determining appropriate frame duration and inter-node waiting time such that packets transmitted from nodes at different distances arrive at the buoy without temporal overlap. The following section formulates these timing constraints and derives the corresponding MAC parameters in closed form.

4.2. Mode Definition

KTEMS benchmarks the DART system, adopting its terminology and parameter settings as references. Table 1 aligns the operation modes of the DART system with similar modes of KTEMS.

Table 1. Modes defined in each system.

DART	KTEMS
Standard mode	Standard mode
Event mode	Report mode
Extended report mode	Data-collecting mode

Figure 5 illustrates the mode transitions between the DART system and KTEMS. Figure 5a shows the DART operation mode. When the event mode is initiated, the extended reporting mode simultaneously starts, during which the system transmits two hours of averaged water-height measurements (i.e., 120 values). The reporting duration of two hours is fixed and cannot be reconfigured. Once the event mode terminates, the extended reporting mode returns to the standard mode. Figure 5b illustrates the mode transition in KTEMS. Each mode will be explained in the following subsections.

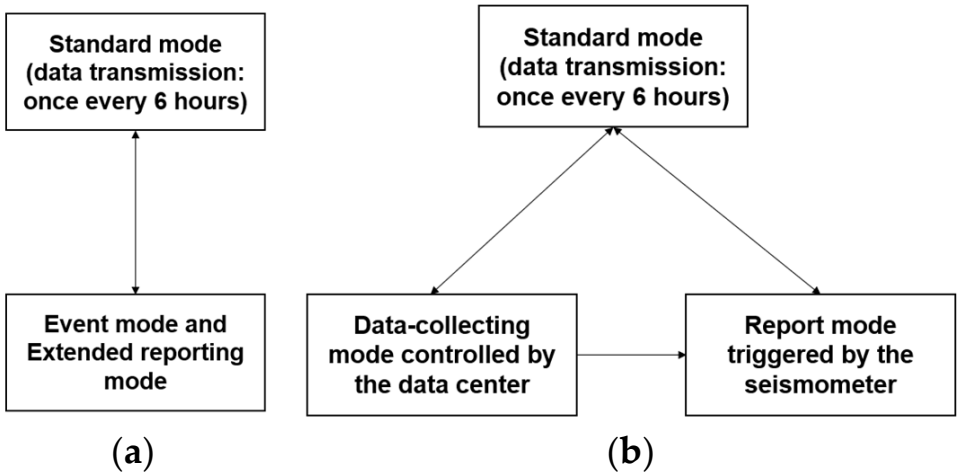


Figure 5. The mode transitions between the DART system and KTEMS: (**a**) DART operation modes, including standard, event, and extended reporting. (**b**) KTEMS operation modes, including standard, data-collecting, and report.

The mode transition of KTEMS is managed through a 4-byte control packet, and the detailed 4-byte bitmap structure is shown in Table 2. The mode indicator field consists of two bits: 00 indicates the standard mode, 11 the report mode, and 01 the data-collecting mode, with 10 reserved for future use. In addition, the data type field, defined by two bits, specifies the source of seismic data: 00 represents seismic data only, 01 indicates seismic data combined with SN1, 10 with SN2, and 11 with both SN1 and SN2. A mode change indicator bit is used to specify whether a mode transition has occurred. In addition, the data-collecting duration field is defined by three bits, allowing the selection of eight options in 15 min increments (i.e., 15, 30, 45, ... 120 min) for the data-collecting duration. This duration is intentionally set shorter than that of the DART extended report mode to reduce power consumption. The detailed ARQ process is currently under investigation and will be addressed in future work.

Table 2. Control packet structure.

Bit	Value	Definition
1–2	Mode indicator	00: standard mode 01: data-collecting mode 10: reserved 11: report mode
3–4	Data type	00: seismic data 01: seismic data + SN1 10: seismic data + SN2 11: Seismic data + SN1 + SN2
5	Mode change	1: changed 0: continued
6–8	Data-collecting duration	000-111: 15 min increments
9–16	ARQ	ARQ information for seismometer
17–27	ARQ	ARQ information for SN1
28–32	ARQ	ARQ information for SN2

In the DART system, DART I supported only one-way communication from the tsunameter to the buoy and subsequently to the data center. Beginning with DART II, bidirectional communication was introduced, enabling the data center to trigger the event mode remotely. Although publicly available technical documents do not specify the detailed timing process for this operation, it can be reasonably inferred that the tsunameter must periodically remain in a listen state to receive such commands.

Similarly, KTEMS incorporates a listen state at each node (seismometer, SN1, and SN2). With this fixed network configuration, the locations of the nodes are preconfigured prior to deployment. Consequently, the seismometer, SN1, and SN2 can calculate the timing of the control packets and enter the listen state whenever control packets are expected.

The required duration for which the seismometer must remain in the listen state can be calculated as follows: for example, assuming a control packet size of 32 bits and a channel data rate of 1250 bps, the corresponding listen state period is (32/1250) = 25.6 ms. Because underwater network protocols must minimize energy consumption, a smaller control packet size is advantageous. Conversely, the buoy, having sufficient power through solar charging, is assumed to remain in the listen state when not transmitting or receiving. More details will be discussed in Section 5.2.

From a usability perspective, the proposed system is designed to operate in real time in the context of tsunami early warning. The system continuously monitors seismic and pressure data and supports event-driven reporting, in which abnormal measurements immediately trigger data transmission to the surface buoy and onward to the warning center. The proposed MAC protocol is frame-based and delay-aware, providing bounded and predictable communication latency rather than best-effort delivery. While the system does not aim at hard real-time guarantees at the physical layer, the end-to-end latency is well within the time scale required for tsunami early warning, which typically ranges from several seconds to a few minutes.

4.3. Report Mode

In the DART I system, the occurrence of an event mode is determined by the tsunameter. When the difference between the predicted water column height from the algorithm and the observed water column height exceeds a predefined threshold (typically in the range of 30–90 mm), an alert signal is promptly transmitted. Because the tsunameter

samples the water height at 15 s intervals, the data from the immediately preceding 15 s are transmitted upon event detection as an alert signal. The generated alert signal activates the modem installed on the buoy, thereby establishing immediate communication between the tsunameter and the data center. The requirement of the DART system is that the alert is delivered to the data center within three minutes [21]; once the tsunameter transmits an alert, the event mode is activated. During this mode, the data sampled over a 15 min interval are aggregated and continuously transmitted.

A distinctive feature of the DART system is the concurrent initiation of the extended-reporting mode together with the event mode. The two modes operate independently in parallel: the event mode reports short-term (15 min) data, whereas the extended-reporting mode transmits one-minute averaged values over a longer period (120 min) to continuously monitor tsunami wave propagation. Both modes are terminated immediately once the difference between the predicted and observed water column height values decreases below the predefined threshold, at which point the system returns to the standard mode. During this process, the transmitted data contain overlapping information across the two modes, introducing redundancy.

This limitation arises from the absence of higher layer control for transmission scheduling, because nodes transmit data only according to predefined fixed rules. While this approach is structurally simple, it can result in data remaining queued before transmission, thereby increasing latency. To address this limitation, the MAC protocol of KTEMS has been designed such that the two modes do not operate simultaneously but are activated at different times as needed. In KTEMS, a report mode is initiated upon the occurrence of an earthquake, and the initial design of this mode was presented in [31]. This subsection provides a summary of its operation.

Figure 6 illustrates the periodically repeated data transmission procedure of the report mode with the network configuration shown in Figure 4. The diagonal lines represent the propagation of packets in Figure 6 and each node can predict the control packet arrival time since the nodes are fixed and synchronized. All parameters used in Figure 6 are listed in Table 3. In the figure, the buoy and the seismometer communicate simultaneously using Frequency Division Duplexing (FDD) because KTEMS employs a buoy equipped with dual receivers. In particular, the seismometer transmits in the dedicated frequency band highlighted in red as in Figure 4, reflecting the higher importance and real-time nature of seismometer data. In contrast, environmental data are transmitted sequentially using Time Division Duplexing (TDD) with the buoy during data transmission.

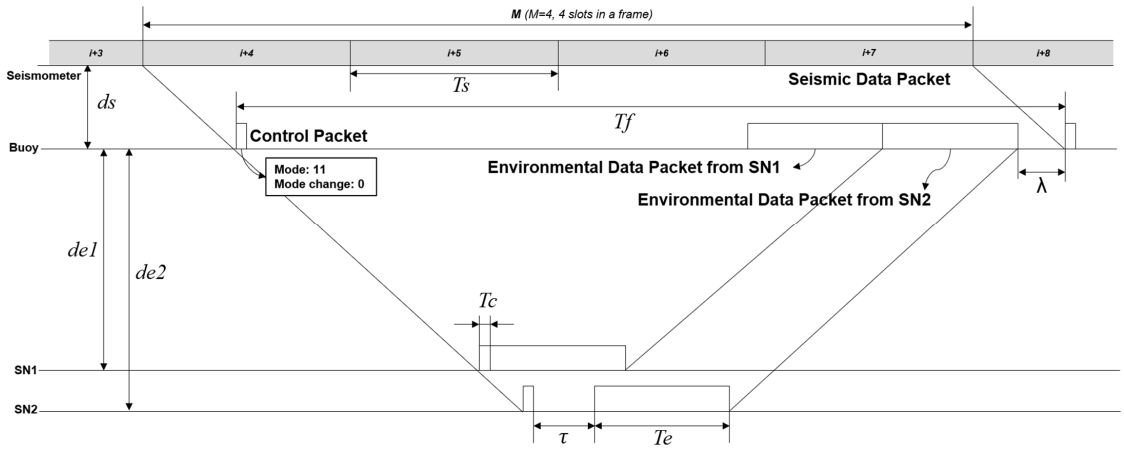


Figure 6. Data transmission procedure in KTEMS during report mode. The seismometer communicates with the buoy using FDD, while environmental nodes (SN1 and SN2) transmit sequentially using TDD after receiving control packets from the buoy.

Table 3. Parameter definitions and units.

Symbols	Definitions
Tf	Frame duration in seconds
Te	Environmental packet duration in seconds
Ts	Seismometer packet duration in seconds
Tc	Control packet duration in seconds
Be	Environmental packet size in bits
Bs	Seismometer packet size in bits
Bc	Control packet size in bits
Rs	Channel data rate in bps at 16 kHz bandwidth
Re	Channel data rate in bps at 4 kHz bandwidth
ds	Distance from the buoy to the seismometer in meters
$de1$	Distance from the buoy to SN1 in meters
$de2$	Distance from the buoy to SN2 in meters
i	Slot number ($i = 0, 1, 2, \ldots$)
τ	SN2 waiting time in seconds
M	Number of packets (slots) in a frame
λ	Rounding up time in Tf for the periodicity

This hybrid duplexing strategy allows KTEMS to efficiently support heterogeneous traffic with different priority levels. While the seismometer benefits from frequency-separated reception to ensure timely delivery of seismic data, the environmental sensor nodes share a single acoustic channel and access the buoy in a time-division manner. Since all underwater nodes operate with half-duplex acoustic modems and the buoy employs a single transmission path for control and feedback signals, a frame-based TDD structure is required to coordinate channel access and prevent collisions among multiple nodes. As the number of participating nodes increases, this shared-channel operation inevitably introduces waiting periods at the buoy, during which no active transmission or reception occurs. Consequently, the design of an efficient MAC protocol becomes critical to minimize channel idle time at the buoy and to maintain high channel utilization, which motivates the advanced protocol design presented in this paper.

As described in Section 3.2, the size of a single seismometer packet is 5000 bits, and each packet is transmitted within a one-second time slot. To improve underwater communication efficiency, M slots are grouped into a single frame. This approach is consistent with the DART system, which employs the XMODEM protocol, where a single packet is divided into multiple blocks. Once M slots are received at the buoy, a control packet is sent, containing both operational information and ARQ information as shown in Table 2. A frame consists of M slots, and its duration is expressed as

$$Tf = MTs \tag{2}$$

where $Ts = Bs/Rs$.

The seismometer can transmit data immediately upon the occurrence of an earthquake, whereas the environmental nodes must first receive a control packet from the buoy before initiating transmission. In this context, the control packet serves as a trigger for data transmission from the environmental nodes. The sensor node closest to the buoy transmits its data immediately after receiving the control packet, while the second sensor node transmits after a predefined delay time, denoted as τ. This delay τ is computed by the protocol as a function of the node locations, as shown in (3), ensuring that the data from the

two nodes do not overlap when arriving at the buoy and can be received efficiently. Here, c denotes the acoustic-wave propagation speed, approximately 1500 m/s.

$$\tau = Te - 2((de2 - de1)/c) \tag{3}$$

where $de2 \geq de1$, $Te = Be/Re$, and $0 \leq \tau$.

In addition, λ denotes the rounding-up time used to align the frame duration (Tf) with the control message periodicity at the buoy. The value of λ is as shown in (4). In each frame, a control packet is transmitted containing operational information and ARQ fields for SN1 and SN2.

$$\lambda = M \cdot Ts - (Tc + \tau + Te + 2(de2/c)) \tag{4}$$

According to (3) and (4), (2) can also be expressed as (5). The frame duration (Tf) must encompass the control packet, waiting delay, environmental packet transmission, and propagation delay, and is therefore defined as given in (5).

$$Tf = Tc + \tau + Te + 2(de2/c) + \lambda \tag{5}$$

Furthermore, the number of slots (M) is defined using the ceiling operation, as given by (6). This operation determines the number of slots required for the slot-based frame structure based on the minimum frame duration.

$$M = ceil\ (Tf/Ts) \tag{6}$$

To improve the overall channel utilization of the network, [31] investigated the optimization of the packet size generated by the environmental sensor nodes. The optimization of the environmental packet size is defined as given in (7) and directly affects the selection of the frame size (M) in KTEMS. When this optimization is applied to the network configuration shown in Figure 4, the values of M are determined according to the node locations relative to the buoy, with typical values of 4, 5, and 6 [31].

$$|\, de2 - de1 \,| = 0.6Be \tag{7}$$

It is worth noting that the number of slots in a frame is not fixed and that the frame structure illustrated in Figure 6 serves as a representative example for explanatory purposes. Even when the optimal value of M is determined to be 4 for a given network geometry, the protocol can still operate correctly with a larger frame size, such as $M = 5$ or $M = 6$. However, using a frame size larger than the optimal value does not improve performance and instead results in reduced channel utilization. This reduction is not caused by the presence of explicit idle slots in the frame, since all slots remain allocated, but rather by increased idle time of the acoustic channel at the buoy. As the frame length exceeds the optimal point, the buoy experiences longer waiting periods without active transmission or reception, resulting in inefficient use of the available channel resources. (The optimal number of slots as a function of SN1 distance can be observed in Section 5.1).

4.4. Standard Mode

The standard mode refers to the normal operating mode when no earthquake occurs. In the DART system, the tsunameter transmits the data stored in its onboard computer to the buoy every six hours. Because data collected during non-tsunami periods are relatively less important for early warning, only the data from the final one-hour interval are transmitted to improve energy efficiency (four 15 min-average values). This reporting procedure also serves to verify the proper operation of the system.

KTEMS is designed with a structure fundamentally similar to that of the DART system, but with additional requirements considered as discussed in Section 3. The protocol operation of KTEMS in the standard mode is illustrated in Figure 7. The seismometer transmits three frames every six hours and the buoy transmits a control packet after each frame. Because the buoy remains in an active state at all times, both transmission and reception are always available. The seismometer transitions to the active state once every six hours to transmit three frames while simultaneously receiving the corresponding control packets. SN1 and SN2 enter the listen state once per frame. Upon receiving three consecutive control packets, the final control packet in the sequence initiates data transmission from SN1 and SN2.

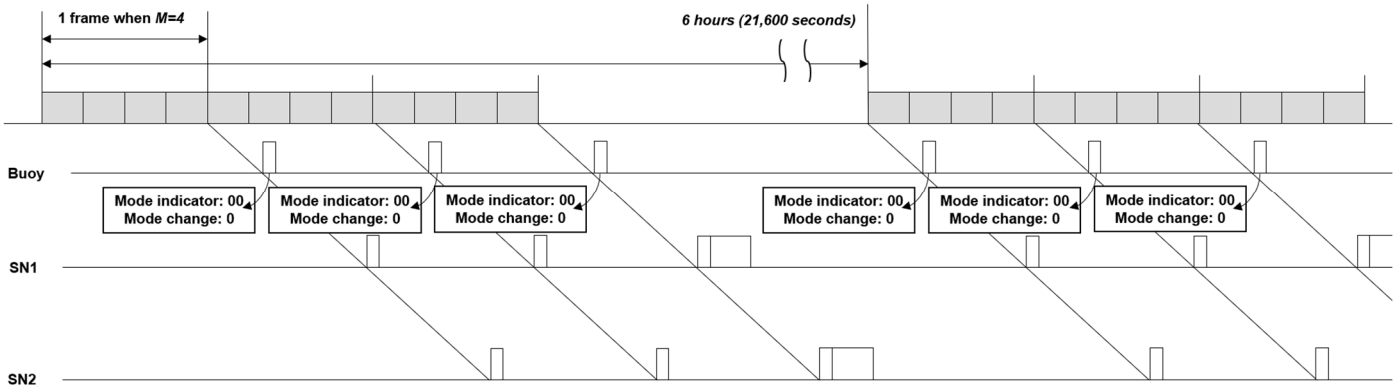


Figure 7. Protocol operation of KTEMS in standard mode. The seismometer transmits three frames every six hours, with the buoy transmitting a control packet after each frame. SN1 and SN2 enter the listen state once per frame after receiving three consecutive control packets; the final packet then triggers environmental data transmission.

Unlike DART, which transmits water column height information, KTEMS transmits raw seismometer data. Therefore, instead of transmitting one hour of data, the system must account for the characteristics of seismic waves. One characteristic of the waves is the short detection window required for earthquake identification, which is typically achieved using the Short-Term Average/Long-Term Average (STA/LTA) algorithm [32]. In this method, the STA window is generally set to approximately 2–3 s, while the LTA window is set to approximately 5–10 s [33–35]. In this study, the STA/LTA algorithm is referenced solely as a representative example to illustrate the typical time scale required for seismic event detection, rather than as a detection method implemented or optimized in the proposed system. Accordingly, KTEMS operates in a three-frame transmission mode to provide a sufficient temporal span for representative short-window seismic detection schemes. If a longer observation window is required by a specific detection algorithm or operational policy at the data center, the system can accommodate this by transmitting additional frames without modifying the underlying MAC design.

The environmental data from SN1 and SN2 are also delivered to the buoy once every six hours. This design choice follows the DART system, in which reporting periodicities are aligned across different data types. In DART-based tsunami early warning systems, tidal information is sampled at 15 min intervals and reported to the warning center at the same periodicity as water column height measurements. Although the official literature does not explicitly state the rationale for this interval, it is generally inferred that aligning the two reporting periodicities facilitates direct comparison between tidal variations and observed water column data. Such alignment not only simplifies data interpretation but also enhances the reliability of anomaly detection during non-tsunami periods.

4.5. Transition from Standard Mode to Report Mode

The seismometer can initiate a transition to the report mode at any time, as illustrated in Figure 8. To signal this transition, a 0.5 s packet (equivalent to a half-slot), similar to the alert signal in DART, is transmitted to the buoy. Because the buoy remains active at all times, it can receive alert signals at any moment. As soon as the buoy receives the alert, it sends an out-of-schedule control packet, whose propagation is indicated as the dotted diagonal line in Figure 8. This control packet contains the mode field set to 11, but SN1 and SN2 cannot switch to the report mode because they are not in the listen state. At this stage, the system remains in the standard mode, and the mode change bit is set to 0. The seismometer continues transmitting data in the next slot, while the buoy sends regular control packets at the frame timing. The control packet transmitted after the current frame triggers the mode changes for SN1 and SN2; therefore, the mode change bit is set to 1 to indicate that the entire system is now in the report mode. Once this packet is received, SN1 and SN2 begin transmitting one data packet per frame. When the report mode terminates, the seismometer automatically reverts to the standard mode. If no packets are received, the buoy also returns to the standard mode, resets the mode field to 00, and sets the mode change bit accordingly. Upon receiving this control packet, SN1 and SN2 revert to the standard mode and transmit one data packet every six hours.

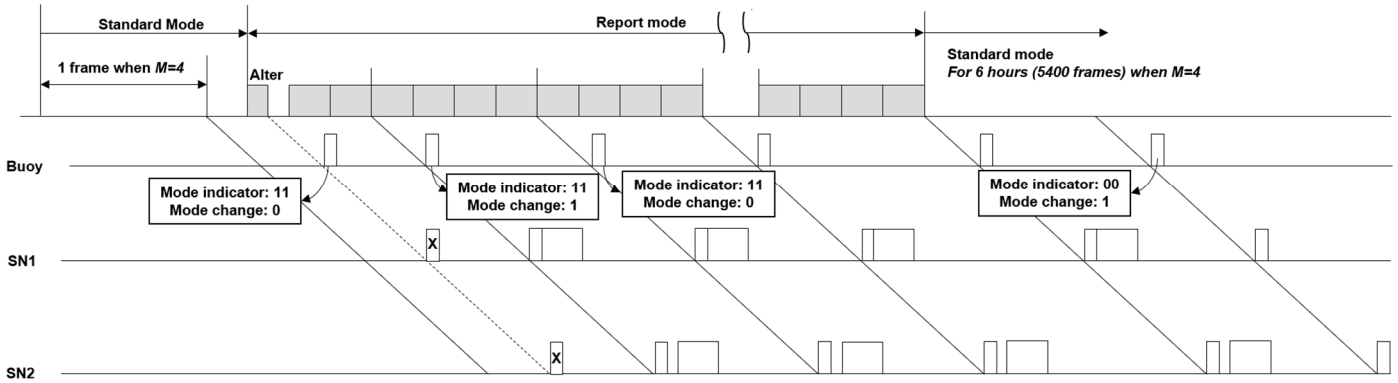


Figure 8. Transition from standard mode to report mode in KTEMS. The seismometer initiates the transition by transmitting a half-slot alert packet, after which the buoy begins sending control packets with mode field 11. SN1 and SN2 switch modes only after receiving the control packet with the mode change bit set to 1. When the report mode terminates, the system returns to the standard mode.

4.6. Data-Collecting Mode

The data-collecting mode is designed to acquire long-term datasets from the seismometer and SNs. This mode is inspired by the extended-reporting mode of the DART system, which enables prolonged data collection. The DART system defines its upper-layer protocol using a modified XMODEM and therefore offers fixed 120 min data collection intervals. In contrast, KTEMS employs a more versatile protocol that allows the selection of both data type and collection duration using two fields in the control packet.

Figure 9 illustrates the operation of the data-collecting mode. When the data type field is set to 11, all three nodes transmit data packets in the same manner as in the report mode. In this example, the data-collecting duration field is configured to 00, corresponding to 15 min of continuous transmission. After the operation completes, the buoy determines whether to remain in the data-collecting mode or to switch to the standard mode. In the case shown in Figure 9, the buoy remains in the same mode with the mode-change bit set to 0. However, the data type field is changed to 10, causing SN1 to stop transmitting data packets while SN2 continues transmission. During the operation, the buoy can dynamically update

the data type; for instance, when the data type is changed to 01, SN1 begins transmission whereas SN2 ceases.

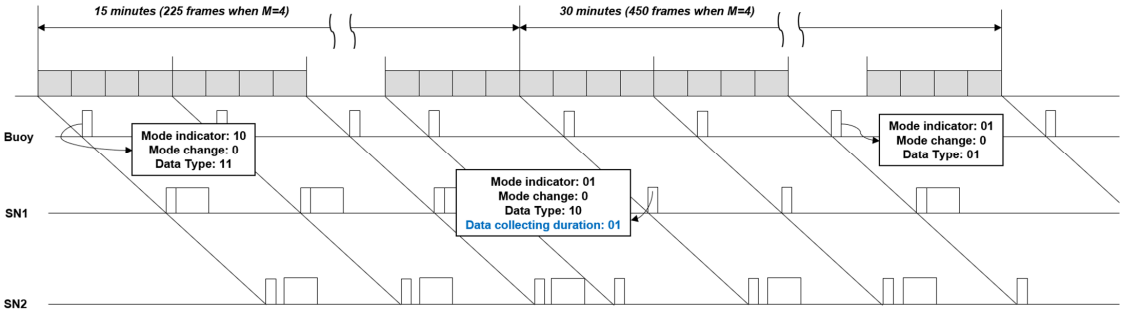


Figure 9. Data-collecting mode of KTEMS. The buoy initiates the mode by sending a control packet that specifies both the data type and the collection duration. Nodes then transmit data accordingly.

In KTEMS, the data-collecting mode operates independently rather than in parallel with the report mode. This separation is necessary because, in the report mode, alert messages must reach the data center much faster than the maximum three-minute latency guaranteed by DART. By decoupling the data-collecting mode from the report mode, KTEMS minimizes queuing delays and thereby reduces the latency of urgent data transmissions.

Energy consumption is also managed through the data-collecting duration field specified in the control packet. This field allows for a significantly shorter collection period compared with that of the DART system. Nevertheless, KTEMS supports consecutive data-collecting operations, enabling continuous data transmission for durations exceeding two hours when required.

4.7. Transition from Standard Mode to Data-Collecting Mode

The transition from the standard mode to the data-collecting mode is initiated by the data center rather than by the seismometer. When additional measurements are required, the data center activates the data-collecting mode through the buoy. Figure 10 illustrates this transition process. When the buoy transmits a control packet with the mode field set to "10" and the mode-change bit set to 1, all three nodes in the listen state receive the packet. This control packet also includes information on the data type and data-collecting duration, based on which the nodes adjust their operation. The seismometer data are always collected, whereas SN1 and SN2 can be selectively activated (SN1 only, SN2 only, both, or neither). Once the data-collecting duration expires, all nodes automatically revert to the standard mode if no further request is received from the data center.

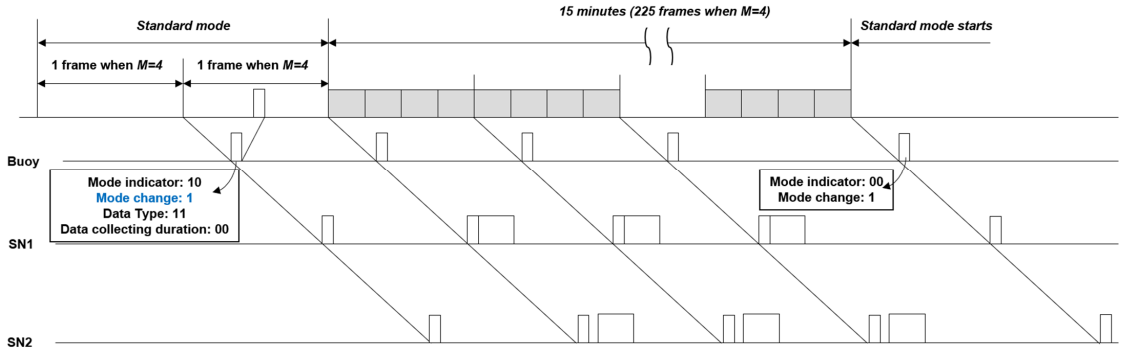


Figure 10. Transition from standard mode to data-collecting mode in KTEMS. The buoy initiates the mode by transmitting a control packet with mode field 10, mode change bit 1, and data type and duration fields. During data-collecting mode, seismometer and selected SNs transmit data for the specified duration, after which the system automatically reverts to the standard mode.

4.8. Transition from Data-Collecting Mode to Report Mode

If an earthquake occurs during the data-collecting mode, the seismometer immediately triggers a transition to the report mode. Figure 11 illustrates this mode transition, which follows a procedure similar to that described in Section 4.5. The seismometer generates a half-slot alert packet, and the buoy responds with an out-of-schedule control packet. Although collisions may occur between the data transmitted by SN1 and SN2 and the out-of-schedule control packet, such collisions are disregarded because the control packet is given priority in subsequent scheduling. In the next regular control packet, the buoy updates the mode indicator and mode change bit fields to reflect the transition to the report mode and then broadcasts this packet. Upon receiving this packet, SN1 and SN2 recognize the report condition and consequently switch to the report mode.

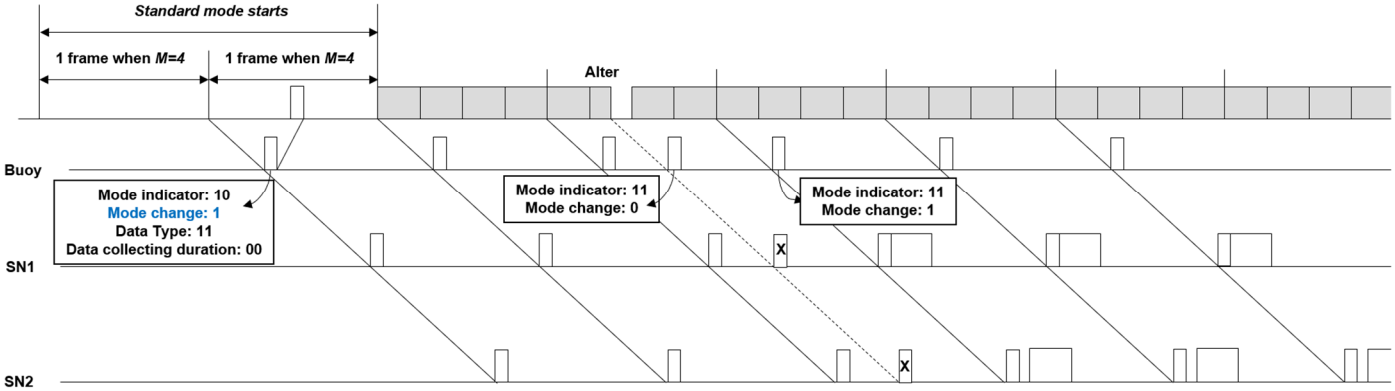


Figure 11. Transition from data-collecting mode to report mode in KTEMS. When an earthquake is detected during data collection, the seismometer transmits a half-slot alert packet. After the ongoing frame ends, the buoy updates the control packet with mode field 11, prompting SN1 and SN2 to recognize the report condition and switch to the report mode.

5. Theoretical Performance Analysis

This section presents the theoretical performance analysis of KTEMS by comparing it with the DART system under different operational modes. Channel utilization and energy consumption are analytically evaluated and discussed. The parameter values used for evaluating KTEMS are listed in Table 4. As illustrated in Figure 4a, the seismometer is positioned 200 m from the buoy, whereas SN2 is located 2000 m from the buoy. The position of SN1 varies from 200 m to 1040 m [31], and the corresponding channel utilization and energy consumption are calculated accordingly. Tables 3–5 collectively summarize the parameter definitions, analysis settings, and power consumption values used throughout the theoretical evaluation in this study. All performance results presented in the following sections are derived under these parameter assumptions.

Table 4. Analysis parameters used for theoretical evaluation.

Symbol	Parameter Values
Rs	5000 bps
Re	1250 bps
ds	200 m
$de1$	200 to 1040 m
$de2$	2000 m
N	The number of received packets from SNs at the buoy
Bs	5000 bits
Bc	32 bits
c	1500 m/s

5.1. Channel Utilization

Channel utilization, measured at the buoy, is defined as the ratio of the time used for receiving valid data within a frame duration, as given in (8). Because the seismometer continuously transmits data packets in both the report and data-collecting modes, it always achieves the maximum channel utilization. In contrast, since transmissions in the standard mode occur only once every six hours, the channel utilization becomes negligibly small. Therefore, the channel utilization in the standard mode is not further discussed in this paper.

$$\text{Channel utilization } (\eta) = N(Te/Tf) \tag{8}$$

In the previous study [31], the channel utilization of KTEMS in the report mode was investigated under packet-size optimization; the corresponding results are illustrated in Figure 12a. By applying the packet size optimization defined in (7), the number of slots per frame (M) followed the step pattern shown in Figure 12b. The frame size determines the packet latency from SN1 and SN2. The channel utilization (η) exhibits a zig-zag pattern owing to the optimized packet size and the corresponding frame size. The channel utilization in the report mode was predicted to be 0.912 when SN1 was located 290 m from the buoy and 0.64 at 1040 m.

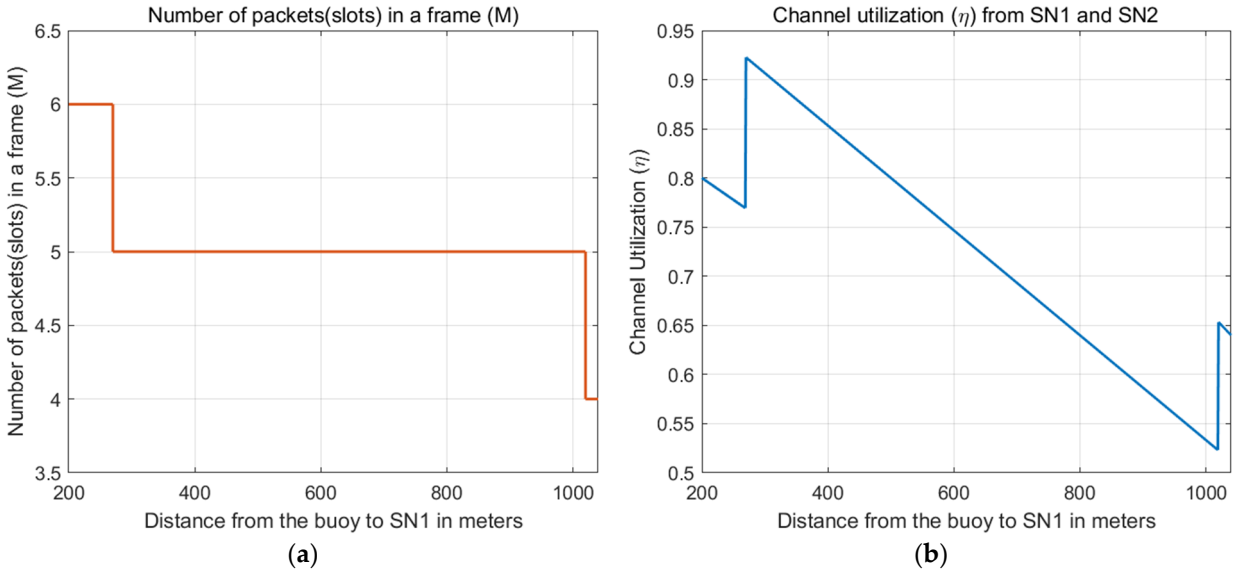


Figure 12. Performance of KTEMS in report mode: (**a**) Frame size (M) as a function of the distance between SN1 and the buoy when the packet size optimization is applied; (**b**) Corresponding predicted channel utilization at the buoy from SN1 and SN2 according to the distance between SN1 and the buoy in the report mode.

Figure 13 illustrates the predicted channel utilization (η) as a function of the distance between the buoy and SN1 ($de1$) under the data-collecting mode. The utilization exhibits a zig-zag pattern similar to that observed in the report mode of KTEMS. In the data-collecting mode, when both SN1 and SN2 transmit data, the same channel utilization as that of the report mode is achieved. When only SN1 or SN2 transmits, the utilization is identical in both cases and equals one-half of the utilization obtained when both nodes transmit. Therefore, when both SN1 and SN2 are active, the data-collecting mode achieves the same channel utilization as the report mode, representing the maximum attainable performance in the network.

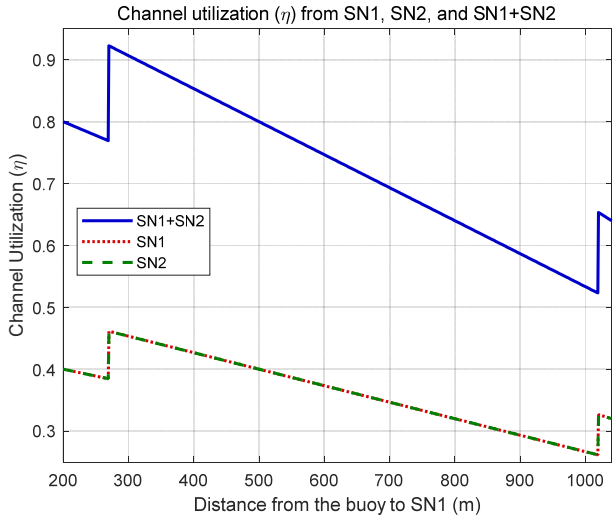


Figure 13. Channel utilization in the data-collecting mode of KTEMS according to the distance between the buoy and SN1, when the data are transmitted by SN1, SN2, or both SN1 and SN2.

5.2. Energy Consumption

In the DART system, detailed power consumption data are not publicly available. Although the specifications of the Benthos ATM-880 acoustic modem (Teledyne Benthos, North Falmouth, MA, USA) [36]—the device used in the tsunameter—were reviewed, state-dependent power figures were not disclosed. Furthermore, the seismometer's exact power characteristics are still under study by the development team (Section 3.2). Therefore, this study refers to [37] and adopts the median values for the KTEMS energy analysis. To minimize distortion caused by skewed data distributions and to better represent typical operating conditions, the median values are used instead of the mean. For example, transmission power consumption ranges from 6 to 975 W, with a median of 11.5 W and a mean of 180 W. The adopted values are summarized in Table 5. These values are intended to provide a reasonable approximation for analyzing energy consumption trends in terms of long-term average behavior and relative performance under typical KTEMS operating conditions, rather than exact absolute power consumption.

Table 5. Power parameters used for energy analysis.

State	Parameter Values
TX	11.5 W
RX	0.6 W
Listen	0.1 W
Sleep	0.01 W

The listen state duration is applicable only in the standard mode, where each node enters the listen state once per frame to receive the control packet from the buoy. Owing to the use of different communication channels, the listen state duration differs between the seismometer and the SNs. Specifically, the listen duration of the seismometer, which operates over a dedicated channel, and that of the SNs, which operate over a shared channel, are given in (9) and (10), respectively:

$$\mathrm{T(listen, seismometer)} = Bc/Rs \tag{9}$$

$$\mathrm{T(listen, SN)} = Bc/Re \tag{10}$$

To clearly distinguish the energy-consumption characteristics associated with different operational modes and node types, the power analysis is presented separately for the standard mode and the data-collecting/report modes, as well as for sensor nodes and the seismometer. Figures 14–17 therefore emphasize complementary, rather than redundant, aspects of KTEMS energy behavior.

5.2.1. Power Consumption in Standard Mode

In the standard mode, as illustrated earlier in Figure 7, all nodes enter the RX state three times to receive control packets from the buoy and switch to the TX state once every six hours for data transmission. Each node enters the listen state once per frame to detect control packets and remains in the sleep state for the remainder of the time.

Figure 14 presents the average power consumption of SN1 over a six-hour cycle, normalized to the hourly average power (mW). The results indicate that SN1 consumes approximately 11 mW on a continuous basis.

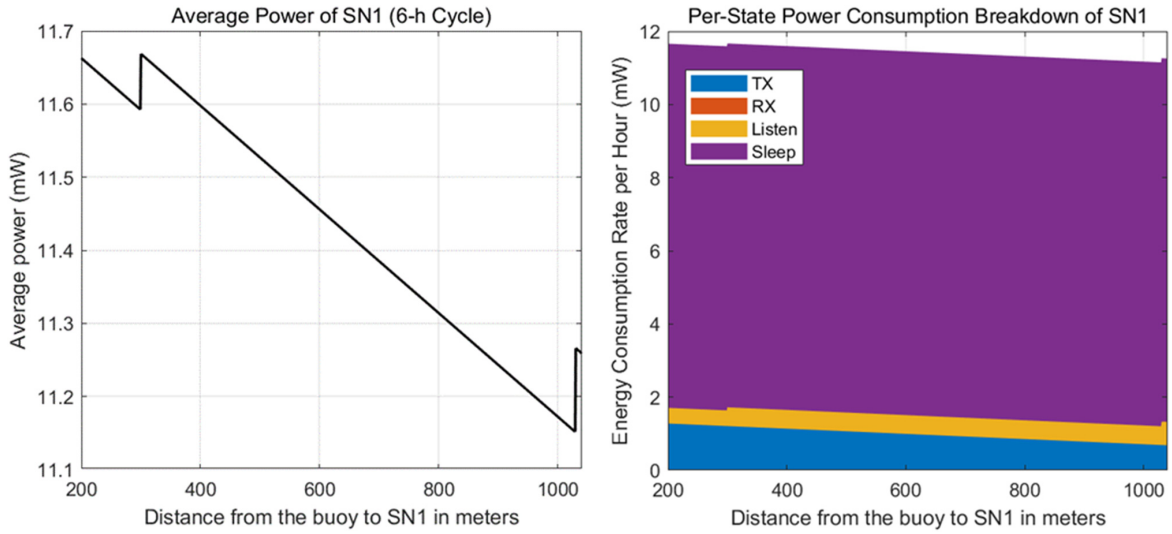


Figure 14. The average power consumption of SNs in standard mode: (**a**) Average power consumption of SN1 in the standard mode of KTEMS over a six-hour operational cycle, normalized to an hourly average power.; (**b**) Energy consumption of SN1 in the standard mode of KTEMS, decomposed by operational states.

Figure 14b further decomposes the average power shown in Figure 14a into the energy consumption associated with each operational state—TX, RX, listen, and sleep. The values are expressed in mW, illustrating the relative contribution of each state to the total average power. Both SN nodes spend the majority of their time in the sleep state, which dominates their overall energy usage profile. Although the nodes periodically enter the listen state, the corresponding energy consumption remains negligible because, in KTEMS, the control packet is designed with minimal functionality and a compact packet size. Because the RX state occurs only three times during a six-hour cycle, its contribution is extremely small and therefore not visible in the figure. By contrast, the TX state, although triggered only once per cycle, accounts for approximately 6.1–11% of the total energy consumption. This relatively higher fraction arises because the data transmission involves several thousand bits, depending on the distance.

For the seismometer, as shown in Figure 7, three frames are transmitted and three control packets are received within each six-hour cycle. In every frame, the seismometer switches to the listen state to confirm control packet reception. Although only three packets

are transmitted during this interval, each packet contains 5000 bits, resulting in significant power consumption in the TX state, as illustrated in Figure 15.

The power consumption in the listen state is identical to that shown in Figure 15b. As illustrated in Figure 4b, the seismometer employs separate transmitter and receiver modules. The TX link operates at a data rate of 5000 bps, whereas the RX link operates at 1250 bps, identical to that of the SNs. Because of this configuration, the power consumption in the RX state remains the same.

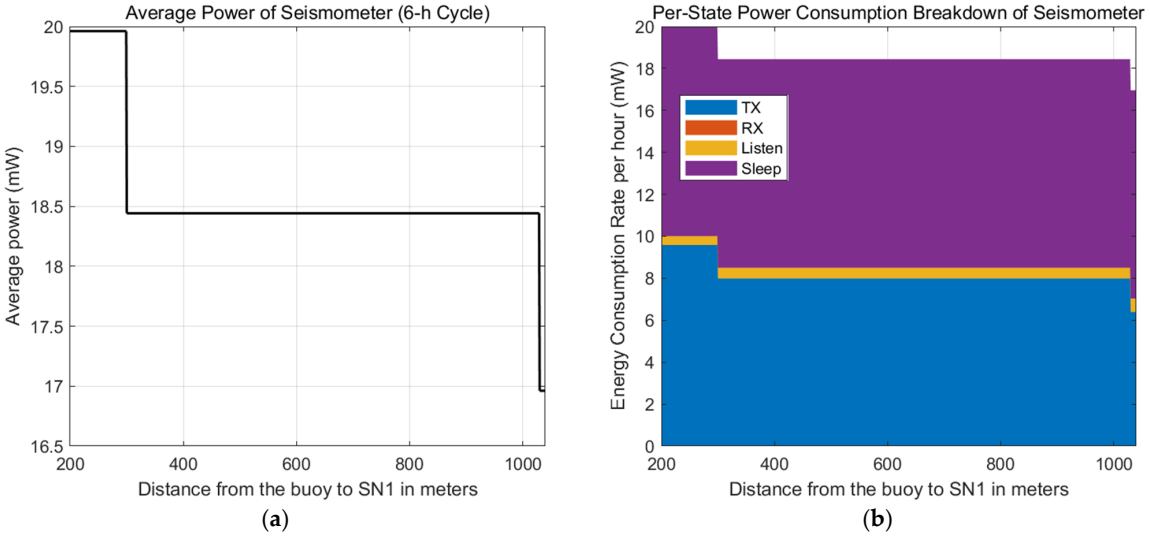


Figure 15. The average power consumption of the seismometer in standard mode: (**a**) Average power consumption of the seismometer in the standard mode of KTEMS over a six-hour operational cycle, normalized to an hourly average power; (**b**) Energy consumption of the seismometer in the standard mode of KTEMS, decomposed by operational states.

5.2.2. Power Consumption in Data-Collecting Mode and Report Mode

During the data-collecting mode, SN1 and SN2 each transmit one data packet and receive one control packet in every frame, remaining in the sleep state for the rest of the time. The listen state is not used in this mode because both SNs are scheduled to transmit data packets. Since the operations of SN1 in the data-collecting and report modes are identical, their energy consumption is analyzed together. Figure 16 presents the power consumption of SN1 when operating in the data-collecting mode for two hours, which is equivalent to a two-hour report-mode operation. The y-axis unit is expressed in watts (W).

The results indicate that most of the energy is consumed in the TX state, whereas the energy consumed in the RX and sleep states is barely visible. When SN1 is located 200 m away from the buoy, two hours of operation in the data-collecting mode correspond to approximately 48 min in tx, 0.5 min in rx, and 71.5 min in sleep. However, because the power consumption in the sleep state is extremely low, it accounts for only about 0.13% of the total energy consumption, which is practically negligible.

The seismometer continuously transmits data packets while simultaneously receiving control packets within each frame duration. Figure 17 illustrates the average power consumption of the seismometer operating in the data-collecting mode. In this mode, only the TX and RX states are active, whereas the sleep and listen states are inactive. Because the control packet is designed with minimal functionality, the power consumption in the RX state remains very low. Although Figure 17a shows slight variations in average power, Figure 17b demonstrates that the overall trend remains nearly constant. This behavior occurs because the seismometer continuously transmits data packets and receives control packets throughout both the report and data-collecting modes.

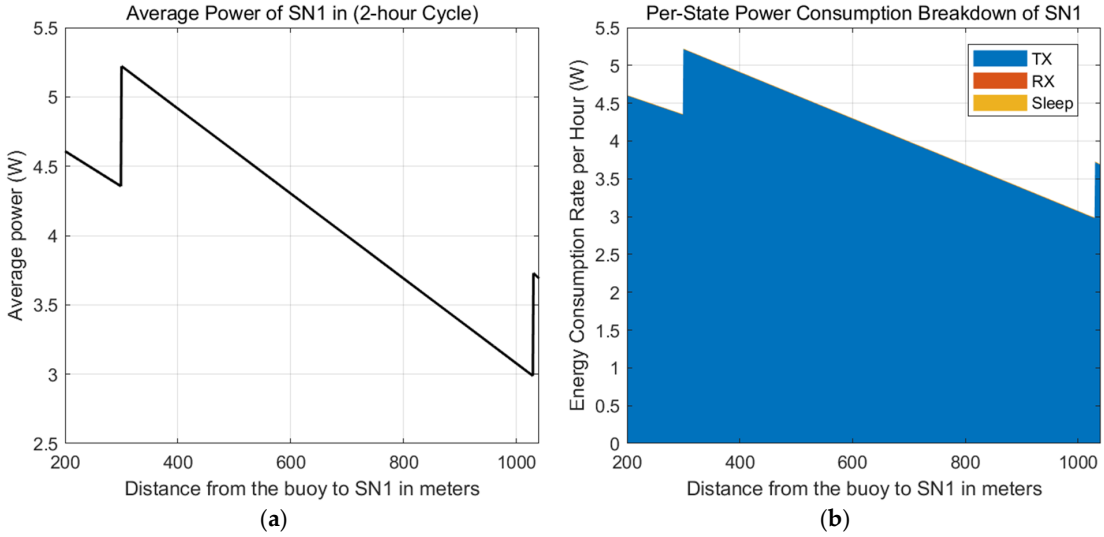


Figure 16. The average power consumption of SNs in data-collecting mode: (**a**) Average power consumption of SN1 in the data-collecting mode or report mode of KTEMS over two hours, normalized to an hourly average power; (**b**) Energy consumption of the SN1 in the data-collecting mode or report mode, decomposed by operational states expressed in W.

In the DART tsunameter shown in Figure 2, the modem is powered by an 1800 Wh battery [36], while the remaining components are supplied by a separate alkaline D-cell battery rated at 1560 Wh [36]. The theoretical battery life of the tsunameter is defined as a target specification rather than a strict operational requirement, with an intended duration exceeding four years. Accordingly, the modem is also assumed to operate for four years. However, the publicly available DART system documentation does not provide detailed information on the modem's state-dependent power consumption. Furthermore, although the Benthos ATM-880 Telesonar modem is reported to be used in the DART system, its product specifications omit such details. Therefore, by dividing the total energy capacity of 1800 Wh by four years, the modem's average power consumption can be theoretically estimated as approximately 51.4 mW.

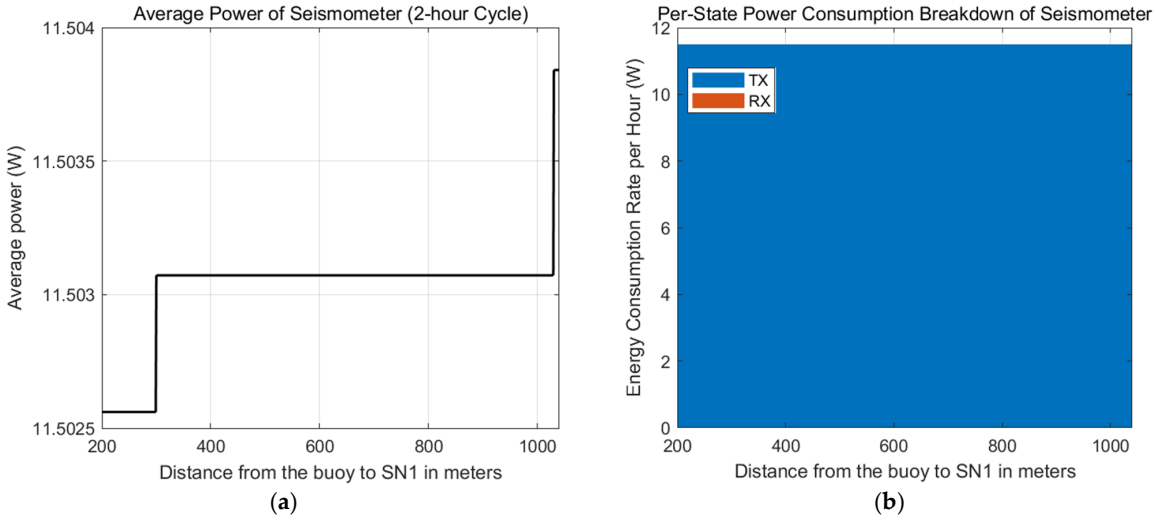


Figure 17. The average power consumption of the seismometer operating in data-collecting mode: (**a**) Average power consumption of the seismometer in the report mode of KTEMS over a two-hour operational cycle, normalized to an hourly average power; (**b**) Energy consumption of the seismometer in the report mode of KTEMS, decomposed by operational states.

If KTEMS employs the same 1800 Wh battery, the estimated lifetime of the seismometer operating in the standard mode can reach approximately 11.3 years (1800 Wh/18 mW $\approx$ 100,000 h) when SN1 is located 600 m from the buoy. Compared with the DART tsunameter, KTEMS reduces the average power consumption to roughly 18 mW through dynamic duty cycling, resulting in a theoretical lifetime nearly three times longer under the same battery capacity.

Considering that major tsunamigenic earthquakes (magnitude $\geq$ 7) occur less than once per decade in the Korean East Sea, the active-reporting period accounts for less than 0.1% of the total operational time. Hence, the estimated lifetime based on standard-mode operation remains practically valid. Because tsunamis are typically generated by earthquakes of magnitude 7 or higher, the probability of issuing a tsunami early warning is relatively low. Therefore, KTEMS is expected to maintain stable operation for well over four years, which further confirms the feasibility of long-term autonomous operation.

All numerical calculations in Figures 12–17 were performed using MATLAB (R2020b, MathWorks, Natick, MA, USA), based on the analytical equations provided in Section 5 The source code used for the calculations is available upon request.

This study focuses on theoretical MAC-level analysis under nominal operating conditions and does not explicitly model environmental effects such as varying sea states or harsh weather conditions. In practice, severe sea states may affect acoustic channel quality, sensor stability, and surface buoy motion, potentially degrading link reliability and increasing packet error rates. Nevertheless, the proposed MAC protocol is designed as a scheduled and delay-aware scheme, which is inherently more robust to long propagation delays and intermittent link degradations than contention-based approaches. While extreme conditions may reduce throughput or increase latency, the fundamental operation of the protocol is expected to remain valid. A detailed evaluation incorporating sea-state-dependent channel models and sea trial measurements is left for future work.

6. Conclusions

This paper presented a theoretical analysis of a MAC protocol designed for KTEMS. Motivated by the limitations of the DART system—which relies on pressure sensors and a one-to-one communication configuration—the proposed protocol integrates seafloor seismometers and supports multi-node acoustic communication tailored to the Korean East Sea environment.

Analytical evaluations were performed in terms of channel utilization and energy consumption. All analytical expressions were verified for internal consistency across operational modes and parameter settings, confirming the theoretical soundness of the proposed framework. The results demonstrate that the KTEMS MAC protocol can sustain multi-year operation with stable performance under underwater acoustic constraints while achieving efficient channel utilization and energy conservation.

Beyond the numerical results, the analysis provides practical engineering insights for the design of underwater networks, particularly in determining optimal node spacing, frame duration, and control packet scheduling to achieve reliability and low latency in coastal monitoring environments. These implications offer valuable guidance for the future implementation of national-scale tsunami and earthquake monitoring infrastructures.

Future work will focus on the following directions: (1) Sea trial measurements will be conducted in the Korean East Sea as part of the ongoing national KIGAM project to collect real underwater acoustic channel data and actual seismometer outputs. These datasets will be used to validate the proposed theoretical model and to confirm latency and energy-consumption predictions under realistic operating conditions. (2) Based on the collected measurements, the behavior of the proposed MAC protocol, including ARQ operation and

retransmission dynamics, will be evaluated and refined to better capture practical underwater channel impairments. (3) The protocol will be further extended by incorporating advanced error-control and adaptive retransmission mechanisms to enhance robustness and reliability for long-term, real-world deployment of the KTEMS. (4) Environmental effects, including varying sea states and harsh weather conditions, will be explicitly incorporated into the analysis by adopting sea-state-dependent underwater acoustic channel models and buoy-motion-aware system modeling. This extension will enable a more realistic assessment of MAC-level performance degradation, including packet error behavior, latency variation, and throughput reduction under adverse operating conditions.

Author Contributions: Conceptualization, S.H.P. and T.I.; methodology, S.H.P.; software, S.H.P.; validation, S.H.P.; formal analysis, S.H.P.; investigation, S.H.P.; resources, S.H.P.; data curation, S.H.P.; writing—original draft preparation, S.H.P.; writing—review and editing, S.H.P.; visualization, S.H.P.; supervision, T.I.; project administration, T.I.; funding acquisition, T.I. All authors have read and agreed to the published version of the manuscript.

Funding: This work was supported by the National Research Foundation of Korea (NRF) grant funded by the Korean Government (MSIT) (NRF-2022M3J9A107887613). This work was supported by the Institute of Information & Communications Technology Planning & Evaluation (IITP) Innovative Human Resource Development for Local Intellectualization program grant funded by the Korean government (MSIT) (IITP-2025-RS-2025-00436765).

Data Availability Statement: The original contributions presented in this study are included in the article. Further inquiries can be directed to the corresponding author.

Conflicts of Interest: The authors declare no conflict of interest.

References

1. BBC News. Tsunami Warnings Across the Pacific. *BBC News*. 30 July 2025. Available online: https://www.bbc.com/audio/play/p0lt4wfc (accessed on 12 October 2025).
2. National Oceanic and Atmospheric Administration (NOAA). The Science Behind Tsunamis Part 1: What is a Tsunami? NOAA: Washington, DC, USA. Available online: https://www.noaa.gov/explainers/science-behind-tsunamis (accessed on 12 October 2025).
3. Lipa, B.; Barrick, D.; Diposaptono, S.; Isaacson, J.; Jena, B.K.; Nyden, B.; Rajesh, K.; Kumar, T.S. High Frequency (HF) Radar Detection of the Weak 2012 Indonesian Tsunamis. *Remote Sens.* **2012**, *4*, 2944–2956. [CrossRef]
4. Lipa, B.; Isaacson, J.; Nyden, B.; Barrick, D. Tsunami Arrival Detection with High Frequency (HF) Radar. *Remote Sens.* **2012**, *4*, 1448–1461. [CrossRef]
5. Heron, M.L.; Prytz, A.; Heron, S.F.; Helzel, T.; Schlick, T.; Greenslade, D.J.; Schulz, E.; Skirving, W.J. Tsunami Observations by Coastal Ocean Radar. *Int. J. Remote Sens.* **2008**, *29*, 6347–6359. [CrossRef]
6. International Tsunami Information Center (ITIC). DART® System Components. ITIC, Honolulu, HI, USA. Available online: https://legacy.itic.ioc-unesco.org/legacy.itic.ioc-unesco.org/index36c9.html (accessed on 12 October 2025).
7. Data Buoy Center (NDBC). National Data Buoy Center. NDBC: Stennis Space Center, MS, USA. Available online: https://www.ndbc.noaa.gov (accessed on 12 October 2025).
8. Korea Meteorological Administration (KMA). Tsunami Case Studies. KMA: Seoul, Republic of Korea. Available online: https://www.weather.go.kr/w/eqk-vol/tsunami/tsunami-case.do (accessed on 12 October 2025).
9. Korea Meteorological Administration (KMA). Domestic Earthquake Search. KMA: Seoul, Republic of Korea. Available online: https://www.weather.go.kr/w/eqk-vol/search/korea.do (accessed on 12 October 2025).
10. Korea Meteorological Administration (KMA). KMA Seismic Observation Network. KMA: Seoul, Republic of Korea. Available online: https://www.kma.go.kr/kma/biz/earthquake_volcano_02.jsp (accessed on 12 October 2025).
11. Korea Institute of Geoscience and Mineral Resources (KIGAM). KIGAM. KIGAM: Daejeon, Republic of Korea. Available online: https://www.kigam.re.kr/english (accessed on 12 October 2025).
12. Ministry of Science and ICT (MSIT). Full-Scale Implementation of the Real-Time Monitoring Technology for Submarine Disasters Project. MSIT: Seoul, Republic of Korea. Available online: https://www.msit.go.kr/bbs/view.do?mId=&bbsSeqNo=94&nttSeqNo=3181774 (accessed on 25 September 2025).
13. Pacific Marine Environmental Laboratory (PMEL). DART 4G. PMEL: Seattle, WA, USA. Available online: https://nctr.pmel.noaa.gov/Pdf/brochures/dart4G_Brochure.pdf (accessed on 12 October 2025).

14. Milburn, H.B.; Nakamura, A.I.; Gonzalez, F.I. Real-time tsunami reporting from the deep ocean. In Proceedings of the OCEANS '96 MTS/IEEE Conference: The Coastal Ocean—Prospects for the 21st Century, Fort Lauderdale, FL, USA, 23–26 September 1996; Volume 1, pp. 390–394.
15. Meinig, C.; Stalin, S.E.; Nakamura, A.I.; Milburn, H.B. *Real-Time Deep-Ocean Tsunami Measuring, Monitoring, and Reporting System: The NOAA DART II Description and Disclosure*; NOAA Technical Report; Pacific Marine Environmental Laboratory (PMEL): Seattle, WA, USA, 2005; pp. 1–15.
16. National Data Buoy Center (NDBC). Deep-Ocean Assessment and Reporting of Tsunamis (DART®) Tsunami Detection Algorithm. Available online: https://www.ndbc.noaa.gov/dart/algorithm.shtml (accessed on 13 December 2025).
17. Meinig, C.; Stalin, S.E.; Nakamura, A.I.; González, F.; Milburn, H.B. Technology developments in real-time tsunami measuring, monitoring and forecasting. In Proceedings of the OCEANS 2005 MTS/IEEE Conference, Washington, DC, USA, 19–23 September 2005; pp. 1673–1679.
18. Mungov, G.; Eblé, M.; Bouchard, R. DART® tsunameter retrospective and real-time data: A reflection on 10 years of processing in support of tsunami research and operations. *Pure Appl. Geophys.* **2013**, *170*, 1369–1384. [CrossRef]
19. Bernard, E.; Titov, V. Evolution of tsunami warning systems and products. *Philos. Trans. R. Soc. A Math. Phys. Eng. Sci.* **2015**, *373*, 20140371. [CrossRef] [PubMed]
20. National Research Council; Division on Earth and Life Studies; Ocean Studies Board; Committee on the Review of the Tsunami Warning and Forecast System. *Tsunami Warning and Preparedness: An Assessment of the U.S. Tsunami Program and the Nation's Preparedness Efforts*; National Academies Press: Washington, DC, USA, 2011.
21. Gonzalez, F.I.; Milburn, H.M.; Bernard, E.N.; Newman, J.C. Deep-Ocean Assessment and Reporting of Tsunamis (DART): Brief overview and Status Report. In Proceedings of the International Workshop on Tsunami Disaster Mitigation, Tokyo, Japan, 19–22 January 1998; Volume 19, p. 2. Available online: https://nctr.pmel.noaa.gov/Pdf/dart_report1998.pdf (accessed on 12 October 2025).
22. Nanometrics. *Pegasus OBS Digital Recorder*; Nanometrics: Kanata, ON, Canada. Available online: https://nanometrics.ca/hubfs/Downloads/Data%20Sheets/pegasus_datasheet_obs.pdf?hsLang=en-ca (accessed on 12 October 2025).
23. Sumy, D.F.; McBride, S.K.; von Hillebrandt-Andrade, C.; Kohler, M.D.; Orcutt, J.; Kodaira, S.; Moran, K.; McNamara, D.; Hori, T.; Vanacore, E.; et al. Long-term ocean observing coupled with community engagement improves tsunami early warning. *Oceanography* **2021**, *34*, 70–77. [CrossRef]
24. Hobin, L.; Kim, Y. A dataset of seismic sensor responses of South Korea seismic stations. *J. Geol. Soc. Korea* **2020**, *56*, 515–524. [CrossRef]
25. Kim, J.; Seo, B.; Han, S.; Choi, K.; Ko, H.; Lee, H. Chirp-based frequency shift keying for underwater acoustic communications. In Proceedings of the 5th International Conference on Ubiquitous and Future Networks (ICUFN), Budapest, Hungary, 2 July 2024.
26. Kwang, Y.C.; Lee, H.; Park, S.H.; Im, T.; Ko, H. OFDM signals underwater experiments and analysis in East Sea of South Korea. In Proceedings of the IEEE 7th International Conference on Information Technology, Information Systems and Electrical Engineering (ICITISEE), Purwokerto, Indonesia, 29 November 2023.
27. Han, S.; Kim, K.; Park, S.H.; Kim, H.; Lee, H. Algorithm to improve synchronization of USBL underwater multipath and Doppler environments. In Proceedings of the IEEE 7th International Conference on Information Technology, Information Systems and Electrical Engineering (ICITISEE), Purwokerto, Indonesia, 29 November 2023.
28. Han, S.; Kim, S.; Ko, H.; Lee, H. Deep learning-based range estimation with sound speed profile. In Proceedings of the IEEE 5th Eurasia Conference on IoT, Communication and Engineering (ECICE), Yunlin, Taiwan, 27 October 2023.
29. Lee, H.; Kim, K.; Choi, T.; Kim, H. Deep learning-based ultra short baseline underwater positioning. In Proceedings of the International Conference on Artificial Intelligence in Information and Communication (ICAIIC), Bali, Indonesia, 20 February 2023.
30. Kim, S.; Han, S.; Park, S.H.; Lee, H.; Im, T. Underwater LFM signal communication analysis from the on-site experiments in West Sea. In Proceedings of the IEEE 7th International Conference on Information Technology, Information Systems and Electrical Engineering (ICITISEE), Purwokerto, Indonesia, 29 November 2023.
31. Park, S.H.; Choi, Y.J.; Im, T.H. Hybrid duplex medium access control protocol for tsunami early warning systems in underwater networks. *Electronics* **2024**, *13*, 4288. [CrossRef]
32. Giridhar, U.S.; Prajapati, N.; Sonkusare, R. Analysis and determination of magnitude of earthquake using STA–LTA algorithm. In Proceedings of the 12th International Conference on Computing, Communication and Networking Technologies (ICCCNT), Kharagpur, India, 6–8 July 2021. [CrossRef]
33. Kumar, S.; Vig, R.; Kapur, P. Development of earthquake event detection technique based on STA/LTA algorithm for seismic alert system. *J. Geol. Soc. India* **2018**, *92*, 679–686. [CrossRef]
34. Katakami, S.; Iwata, N. Enhancing railway earthquake early warning systems with a low computational cost STA/LTA-based S-wave detection method. *Sensors* **2024**, *24*, 7452. [CrossRef] [PubMed]
35. Ho, L.M.; Walter, J.I.; Hansen, S.E.; Sánchez-Roldán, J.L.; Peng, Z. Evaluating automated seismic event detection approaches: An application to Victoria Land, East Antarctica. *J. Geophys. Res. Mach. Learn. Comput.* **2024**, *1*, e2024JH000185. [CrossRef]

36. National Data Buoy Center (NDBC). DART® Design Characteristics/Specifications. NDBC: Stennis Space Center, MS, USA. Available online: https://www.ndbc.noaa.gov/dart/dart2_pc_1.shtml (accessed on 12 October 2025).
37. Zia, M.Y.I.; Poncela, J.; Otero, P. State-of-the-art underwater acoustic communication modems: Classifications, analyses and design challenges. *Wireless Pers. Commun.* **2021**, *116*, 1325–1360. [CrossRef]

Disclaimer/Publisher's Note: The statements, opinions and data contained in all publications are solely those of the individual author(s) and contributor(s) and not of MDPI and/or the editor(s). MDPI and/or the editor(s) disclaim responsibility for any injury to people or property resulting from any ideas, methods, instructions or products referred to in the content.